

# The peculiarities of magnetization processes in layered high-temperature superconductors with ferromagnetic defects under applying of transport current and external magnetic field

V A Kashurnikov, A N Maksimova and I A Rudnev

National Research Nuclear University (Moscow Engineering Physics Institute),  
Moscow Russia

**Abstract.** The Monte-Carlo method was used for study of magnetization processes in 2D layered high temperature superconductors (HTSC) with internal ferromagnetic defects. The magnetization was treated under application of transport current and external dc magnetic field. The voltage-current characteristics (I-V curve) were calculated in presence of external dc magnetic field. A novel S-type I-V curve of the superconductor/ferromagnet system in external magnetic field was demonstrated. It was shown that the S-type nonlinearity is due to the local reversal magnetization of magnetic particles by the field of vortices. The H-T phase diagram which demonstrates the region of existence I-V curve nonlinearity was obtained. The conditions for electromagnetic generation at the region of nonlinearity were found and the frequency of such a generation was estimated.

## 1. Introduction

The value of the critical current is the most important characteristic of the type II superconductors for various electrical engineering applications. The critical current strongly depends on the properties of intrinsic defects. When the current exceeds the critical value, vortices of opposite polarities start to move under the action of Lorentz force and annihilate close to the geometrical centre of the slab. These processes give rise to the power losses, appearance of the voltage on the sample and the transition of the superconductor to the normal state. Therefore it is crucial to investigate the influence of defect structure on transport properties of type II superconductors. Transport properties, phase transitions in vortex lattice, magnetization processes and voltage-current characteristics have been widely investigated in [1-5] for HTSC with nonmagnetic defects by using Monte-Carlo method.

The effect of ferromagnetism on the superconducting state attracted considerable attention in recent years. The ferromagnetic impurities in high-temperature and low-temperature superconductors were investigated to improve current-carrying ability, and the interaction of ferromagnetic phases with superconductivity has been used for solve the problem of the coexistence of superconductivity and ferromagnetism in a mixed vortex state. An enhancement of vortex pinning by a magnetic nanoparticle is expected due to rise of the energy of magnetic particles in the field of vortex in addition to conventional nonmagnetic part of interaction. HTSC samples on ferromagnetic substrates and HTSC with intrinsic ferromagnetic defects were investigated in the papers [6,7] in which the magnetization curves were obtained. The nonlinear interaction between ferromagnetic particles and superconductor was demonstrated. The force of interaction of a single vortex line with a spherical magnetic nanoparticle of arbitrary radius was calculated [8]. Analysis of the behavior of ferromagnetic Gd in Nb [9] showed that the pinning force is due to the hysteretic loss for magnetization reversal.

The aims of this paper are investigation of transport properties of HTSC sample with ferromagnetic defects as internal pinning centers and a correct calculation of voltage-current characteristics in the presence of external dc magnetic field. Here, we represent the results of calculation of VACH by using the Monte-Carlo method. Orientation of ferromagnetic nanoparticles' easy axes and values of magnetic anisotropy parameter were taken into account, the case of periodic lattice of ferromagnetic defects was analyzed for specificity.



## 2. Model

To calculate an equilibrium distribution of vortices, we numerically minimized the Gibbs thermodynamic potential of the 2D vortex system with a varying number of pancake vortices; this potential has the form (see [4,7], where the model and the algorithm are described in details):

$$G = sN\varepsilon + \sum_{i<j} U_{in-plane}(r_{ij}) + s \sum_{i,j} U_p(r_{ij}) + \sum_{i,j} U_{surf}(r_{ij}^{(im)}), \quad (1)$$

where  $\varepsilon$  is a self-energy of vortex,  $s$  is a thickness of a superconducting layer and  $N$  is the number of vortices in the system, the second term describes pair interaction of vortices, the third term takes into account the interaction of vortices with pinning centers and the fourth term describes the interaction of vortices with the surface and the external field. Pancakes in a plane interact with the long-range potential in the following form:

$$U_{in-plane}(r_{ij}) = s \frac{\Phi_0^2}{8\pi^2 \lambda^2} K_0\left(\frac{r_{ij}}{\lambda}\right), \quad (2)$$

where  $r_{ij}$  is a distance between vortices and  $\lambda = \lambda(T) = \lambda(T=0) / \sqrt{1 - (T/T_c)^2}$  is the magnetic field penetration depth,  $K_0(x)$  is a Bessel function and  $T_c$  is a superconducting critical temperature.

Then we take into account an ensemble of ferromagnetic nanoparticles in the bulk of superconductor. The magnetic part of the pinning force was calculated as an energy of interaction of magnetic dipole of ferromagnetic defect with the field of Abrikosov vortex. Gibbs potential of the ferromagnetic particle has a form:

$$U_p = U + U_{pm} + U_{pn}, \quad U_{pm} = -\mu H_v, \quad (3)$$

$\mu$  is the projection of the magnetic moment onto the direction of the external field,  $H_v$  is the field produced by the vortex at the point of location of the particle. In our calculations, we choose  $\mu \approx 10^4 \mu_0$ .  $U_{pn}$  is the nonmagnetic part of the interaction,  $U$  is a part of particle's energy, not associated with vortices.  $\mu_0$  is the Bohr magneton.  $U$  value includes the particle's energy in the field of Meissner current and the energy of magnetic anisotropy (in [7,10] the magnetization processes in assembly of ferromagnetic nanoparticles in the field of Abrikosov vortices are described in details). The magnetization of ferromagnetic nanoparticles depends on the mutual orientation of particle's easy axes and the direction of external magnetic field. In this paper easy axes are parallel to an external field.

The interaction of vortex with Meissner current is an inverse work of Lorentz force on a vortex to move it from the surface deep into the sample:

$$U_m = \frac{\Phi_0}{4\pi} \left[ H_0 \left( 1 - \frac{ch(x/\lambda)}{ch(d/2\lambda)} \right) + H_l \left( \frac{sh(x/\lambda)}{sh(d/2\lambda)} \mp 1 \right) \right] \quad (4)$$

$H_0$  - is an external magnetic field,  $H_l = 2\pi I / c$  - magnetic field at the sample's surface produced by transport current,  $I$  is a total transport current through the sample cross section,  $d$  - sample's width. One should take "-" before unity when vortex appears at  $x > 0$  (right side) and "+" otherwise [4].

Calculations were done at 1-10 K, for typical characteristics of  $Bi_2Sr_2CaCu_2O_{8-\delta}$ :  $\lambda(0) = 180$  nm,  $\xi(0) = 2$  nm,  $T_c = 84$  K. The anisotropy parameter was chosen  $K = 0.1 \cdot 10^7$  erg/cm<sup>3</sup>. Ferromagnetic nanoparticles have the size  $\sim \xi$  which corresponds to magnetic moment  $\mu \sim 10^4 \mu_B$ .

## 3. Results and discussion

The current-voltage characteristics were obtained by using method developed in [5]. When a viscous flow of vortex lines is established, the dynamic component of the losses per unit volume

$W = jE$  may be obtained by counting the number of annihilated vortex-antivortex pairs. In our calculations, we defined the critical current as the current at which the voltage per unit length in the sample is  $E=0.1 \mu V/cm$ . Figure 1 represents the voltage-current characteristics for the sample with ferromagnetic defects at different values of external dc magnetic field.

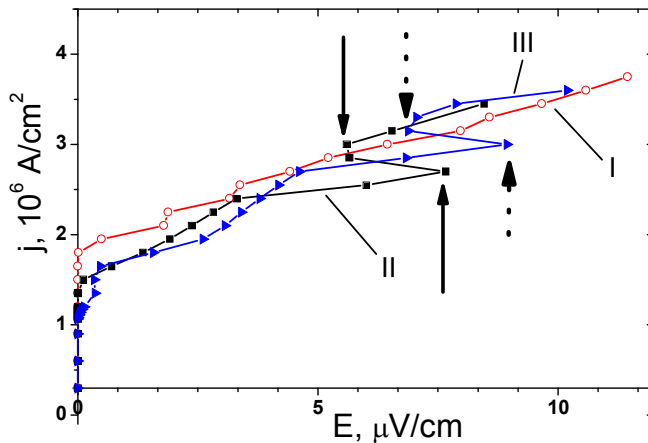


Figure 1. The voltage-current characteristics at fixed concentration of magnetic defects  $c = 1,06 \cdot 10^9 cm^{-2}$  and different values of external field. I –  $H=200$  Gs, II –  $H=400$  Gs, III –  $H=500$  Gs.  $T = 1K$ , much smaller than  $T_c = 84K$  and Curie temperature. The regions of S-type nonlinearity are marked with arrows.

As it is replotted in Figure 1, the S-type nonlinearity appears while external magnetic field increases. In contrast to the case with nonmagnetic defects, the orientation of particles magnetic moments is not fixed and depends on local magnetic fields and the field of transport current. As we can see from figure 1, the nonlinearity that appears at lower current when magnetic field is smaller and the nonlinearity is absent below some critical value. The analysis of vortex configurations and magnetization of defects shows that the instabilities on the ac-characteristics correlate with drastic changes in magnetization of defects. Before the nonlinearity the vortex concentration is not enough for reorientation of magnetic moments and the effective concentration of pinning centers is small.

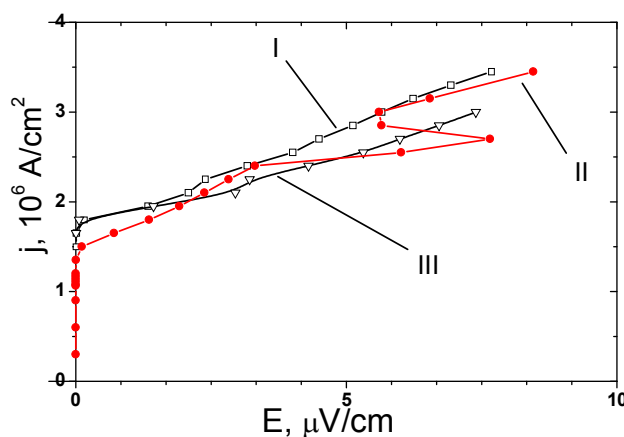


Figure 2. I-V curves at different concentrations of nonmagnetic defects: I – nonmagnetic,  $c = 7.5 \cdot 10^8 cm^{-2}$ , II - magnetic,  $c = 1.06 \cdot 10^9 cm^{-2}$ , III - nonmagnetic,  $c = 4 \cdot 10^8 cm^{-2}$ . I-V curve for nonmagnetic defects is shown for comparison (2),  $H = 400Gs$ , the depth of potential well of nonmagnetic defects was chosen equal to effective depth of magnetic defects, so that

$$\mu \frac{\Phi_0}{2\pi\lambda^2} \left( \ln \frac{\lambda}{\xi} - 0,28 \right) = 0,02 \text{ eV.}$$

After nonlinearity the magnetic moments are parallel to the magnetization of vortices on the left side and the effective concentration of pinning centers increases. Figure 2 shows two I-V curves for different concentrations of nonmagnetic defects (with pinning force nearly equal to the pinning force

of magnetic defects). The  $j(E)$  curve is always higher for larger defect concentration and at the region of instability the transition from I-V curve for small concentration to I-V curve for higher concentration occurs. This effect is close to the one of the change of defect concentration in systems with high magnetic anisotropy examined in [7]. The analysis of influence of external parameters shows that the nonlinearity shifts to left and concurrently becomes straight at increasing temperature and above certain temperature is absent. Figure 3 shows the H-T phase diagram of the region of existence I-V curve nonlinearity. The temperature threshold at  $T \approx 6K$  is due to magnetization reversal processes in assembly of magnetic particles. At higher temperature the magnetization of the particles becomes more reversible and the reorientation of magnetic moments occurs at lower magnetic fields.

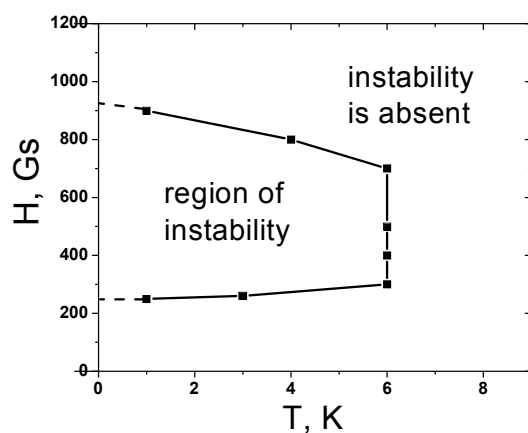


Figure 3. The H-T phase diagram of the region of existence I-V curve nonlinearity. The threshold temperature corresponds to the case when  $T$  is of order of the energy of magnetic anisotropy i.e. thermal fluctuations of magnetic moments become essential.  $KV \sim T$ , from which at the chosen value of magnetic anisotropy parameter  $T \approx 6K$ .

#### 4. Conclusion

In summary, the magnetization of layered HTSC with internal ferromagnetic defects was calculated by Monte-Carlo method taking into account the field of transport current. The voltage-current characteristics in presence of external dc magnetic field were obtained. A novel, S-type of I-V curve was demonstrated. It was shown that the nonlinearity is caused by the local reversal magnetization of magnetic particles by the field of vortices which leads to an abrupt change in effective concentration of pinning centers. The influence of temperature and value of external dc magnetic field on the shape of  $j(E)$  curve was investigated, the H-T phase diagram for the region of existing the nonlinearity was obtained.

#### Acknowledgements

The work was supported by RFBR, Grant **14-22-00098**.

- [1] Kashurnikov V A, Rudnev I A, Gracheva M E, Nikitenko O A 2000 *JETP* **90** (1) 173
- [2] Zyubin M V, Rudnev I A, Kashurnikov V A 2003 *JETP* **96** (6) 1065
- [3] Kashurnikov V A, Rudnev I A, Zyubin M V 2001 *Supercond. Sci. and Techn.* **14**(9) 695
- [4] Odintsov D S, Rudnev I A, Kashurnikov V A 2006 *JETP* **103** (1) 66-76
- [5] Rudnev I A, Odintsov D S, Kashurnikov V A, 2008 *Phys. Lett. A* **372** 3934-3936
- [6] Ilyina E A et al 2010 *Physica C* **470** 877-879
- [7] Kashurnikov V A, Maksimova A N, Rudnev I A 2014 *Physics of the Solid State* **56** (5) 894-911
- [8] Snezhko A, Prozorov T, Prozorov R 2005 *Phys. Rev. B: Condens. Matter* **71** 024527
- [9] Palau A, Parvaneh H, Stelmashenko N A 2007 et al *Phys. Rev. Lett.* **98** 117003
- [10] Prozorov R, Yeshurun Y, Prozorov T, Gedanken A 1999 *Phys. Rev. B* **59** 6956